Table 1. *Fractional atomic coordinates and equivalent isotropic displacement parameters* (Å^2)

$$U_{eq} = (1/3)\Sigma_i\Sigma_j U_{ij} a_i^* a_j^* \mathbf{a}_i.\mathbf{a}_j.$$

	x	y	z	U_{eq}
Pr(1)	0.18380 (2)	0.10391 (5)	0.16958 (4)	0.00889 (6)
Pr(2)	1/2	0.07297 (8)	1/4	0.00996 (9)
Cl	0	0.0271 (4)	1/4	0.0305 (6)
Si	0.3420 (1)	−0.0553 (3)	−0.0251 (2)	0.0087 (3)
O(1)	0.1549 (3)	0.3854 (8)	0.3440 (5)	0.0124 (9)
O(2)	0.2389 (3)	−0.0572 (8)	0.4174 (5)	0.0105 (8)
O(3)	0.0781 (3)	0.3754 (8)	0.0295 (6)	0.0131 (9)
O(4)	0.1420 (4)	−0.2614 (8)	0.1443 (6)	0.015 (1)

Table 2. *Selected geometric parameters* (Å, °)

Pr(1)—Cl	2.8611 (7)	Pr(2)—O(1^{i})	2.551 (5)
Pr(1)—O(1)	2.442 (5)	Pr(2)—O(3^{iv})	2.686 (5)
Pr(1)—O(1^{i})	2.718 (5)	Pr(2)—O(3^{i})	2.686 (5)
Pr(1)—O(2)	2.430 (4)	Pr(2)—O(3^{vi})	2.559 (5)
Pr(1)—O(2^{ii})	2.607 (5)	Pr(2)—O(3^{vii})	2.559 (5)
Pr(1)—O(2^{iii})	2.468 (5)	Pr(2)—O(4^{v})	2.581 (5)
Pr(1)—O(3)	2.509 (5)	Pr(2)—O(4^{ii})	2.581 (5)
Pr(1)—O(4)	2.426 (5)	Si—O(1^{i})	1.625 (5)
Pr(2)—Cl^{iv}	3.510 (3)	Si—O(2^{iii})	1.654 (5)
Pr(2)—Cl^{v}	2.920 (3)	Si—O(3^{vi})	1.631 (5)
Pr(2)—O(1^{iv})	2.551 (5)	Si—O(4^{viii})	1.612 (5)
O(1^{i})—Si—O(2^{iii})	107.2 (3)	Cl^{v}—Pr(2)—Si	105.12 (3)
O(1^{i})—Si—O(3^{vi})	105.7 (3)	Cl^{v}—Pr(2)—Si^{ix}	105.12 (3)
O(1^{i})—Si—O(4^{viii})	118.3 (3)	Cl^{v}—Pr(2)—Si^{x}	92.03 (3)
O(2^{iii})—Si—O(3^{vi})	106.2 (3)	Cl^{v}—Pr(2)—Si^{xi}	92.03 (3)
O(2^{iii})—Si—O(4^{viii})	109.1 (3)	Si—Pr(2)—Si^{ix}	149.76 (5)
O(3^{vi})—Si—O(4^{viii})	109.7 (3)	Si—Pr(2)—Si^{x}	90.72 (5)
Cl^{iv}—Pr(2)—Cl^{v}	180.00 (6)	Si—Pr(2)—Si^{xi}	88.22 (5)
Cl^{iv}—Pr(2)—Si	74.88 (3)	Si^{ix}—Pr(2)—Si^{x}	88.22 (5)
Cl^{iv}—Pr(2)—Si^{ix}	74.88 (3)	Si^{ix}—Pr(2)—Si^{xi}	90.72 (5)
Cl^{iv}—Pr(2)—Si^{x}	87.97 (3)	Si^{x}—Pr(2)—Si^{xi}	175.95 (5)
Cl^{iv}—Pr(2)—Si^{xi}	87.97 (3)		

Symmetry codes: (i) $\frac{1}{2}-x, y-\frac{1}{2}, \frac{1}{2}-z$; (ii) $\frac{1}{2}-x, \frac{1}{2}+y, \frac{1}{2}-z$; (iii) $x, -y, z-\frac{1}{2}$; (iv) $\frac{1}{2}+x, y-\frac{1}{2}, z$; (v) $\frac{1}{2}+x, \frac{1}{2}+y, z$; (vi) $\frac{1}{2}-x, \frac{1}{2}-y, -z$; (vii) $\frac{1}{2}+x, \frac{1}{2}-y, \frac{1}{2}+z$; (viii) $\frac{1}{2}-x, -\frac{1}{2}-y, -z$; (ix) $1-x, y, \frac{1}{2}-z$; (x) $1-x, -y, -z$; (xi) $x, -y, \frac{1}{2}+z$.

The positions of the Pr atoms were located in space group *C*2/*c* by direct methods (Gilmore, 1983). The coordinates of the remaining atoms were found in succeeding difference Fourier syntheses. To apply the radial part of the absorption correction, it was assumed that the crystal is spherical with a radius equal to the effective size of the crystal in the direction in which the ψ scans give a transmission factor of 1.0. The structure was refined by full-matrix least-squares methods.

Data collection: *CONTROL* (Molecular Structure Corporation, 1988). Cell refinement: *CONTROL*. Data reduction: *MolEN* (Fair, 1990). Program(s) used to solve structure: *MITHRIL* (Gilmore, 1983). Program(s) used to refine structure: *LSFM* in *MolEN*. Molecular graphics: *ORTEP*II (Johnson, 1976). Software used to prepare material for publication: *GCIF*, local program.

This work was funded by the National Nature Science Foundation of China, the State Key Laboratory of Structure Chemistry and the Natural Science Foundation of Fujian Province.

Lists of structure factors, anisotropic displacement parameters and complete geometry have been deposited with the IUCr (Reference: BR1101). Copies may be obtained through The Managing Editor, International Union of Crystallography, 5 Abbey Square, Chester CH1 2HU, England.

References

Ayasse, C. & Eick, H. A. (1973). *Inorg. Chem.* **12**, 1140–1143.
Chen, J.-T., Guo, G.-C., Huang, J.-S. & Zhang, Q.-E. (1995). In preparation.
Fair, C. K. (1990). *MolEN. An Interactive Intelligent System for Crystal Structure Analysis*. Enraf–Nonius, Delft, The Netherlands.
Gilmore, C. J. (1983). *MITHRIL. Computer Program for the Automatic Solution of Crystal Structures from X-ray Data*. Department of Chemistry, Univ. of Glasgow, Scotland.
Gravereau, P., Es-Sakhi, B. & Fouassier, C. (1988). *Acta Cryst.* C**44**, 1884–1887.
Gravereau, P., Es-Sakhi, B. & Fouassier, C. (1989). *Acta Cryst.* C**45**, 1677–1679.
Johnson, C. K. (1976). *ORTEP*II. Report ORNL-5138. Oak Ridge National Laboratory, Tennessee, USA.
Molecular Structure Corporation (1988). *CONTROL. An Automatic Package for Rigaku AFC Single-Crystal Diffractometers*. MSC, 3200 Research Forest Drive, The Woodlands, TX 77381, USA.
Yamada, H., Kano, T. & Tanabe, M. (1978). *Mater. Res. Bull.* **13**, 101–108.

Acta Cryst. (1995). C**51**, 2473–2476

Potassium Vanadium Selenite, $K(VO_2)_3(SeO_3)_2$

WILLIAM T. A. HARRISON, LAURIE L. DUSSACK AND ALLAN J. JACOBSON

Department of Chemistry, University of Houston, Houston, TX 77204-5641, USA

(*Received* 15 *March* 1995; *accepted* 22 *June* 1995)

Abstract

The hydrothermal synthesis and single-crystal structure of potassium vanadium(V) selenite, $K(VO_2)_3(SeO_3)_2$, are reported. $K(VO_2)_3(SeO_3)_2$ is a layered phase based on a hexagonal tungsten-oxide-like array of corner-sharing VO_6 octahedra capped by Se atoms, and is isostructural with $NH_4(VO_2)_3(SeO_3)_2$.

Comment

$K(VO_2)_3(SeO_3)_2$, which is isostructural with $NH_4(VO_2)_3(SeO_3)_2$ (Vaughey, Harrison, Dussack & Jacobson, 1994), is another example of a phase built up from sheets of vertex-sharing VO_6 octahedra like those of hexagonal tungsten oxide (HTO) (Figlarz, 1989). This layer configuration results in octahedral 'three-rings' and 'six-rings' (Fig. 1). Half the three-rings on each side of the V/O layer are capped by Se atoms (as $[SeO_3]^{2-}$ selenite groups), *i.e.* capping occurs on both faces of the infinite VO_6 sheets (Fig. 2). The K cations, which occupy six-coordinate sites in the inter-layer region, provide charge balancing.

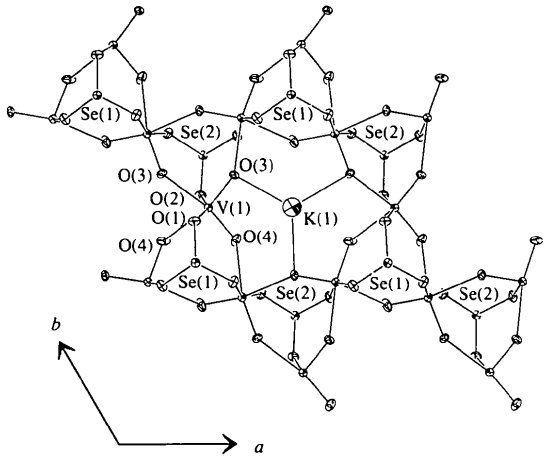

Fig. 1. View down [001] showing the hexagonal tungsten-oxide-like layer in $K(VO_2)_3(SeO_3)_2$. In this view, all the Se(1) atoms project upwards and all the Se(2) atoms downwards. O(3) and O(4) form the 'three-ring' links and also alternate around the 'six-rings'. Displacement ellipsoids are drawn at the 50% probability level.

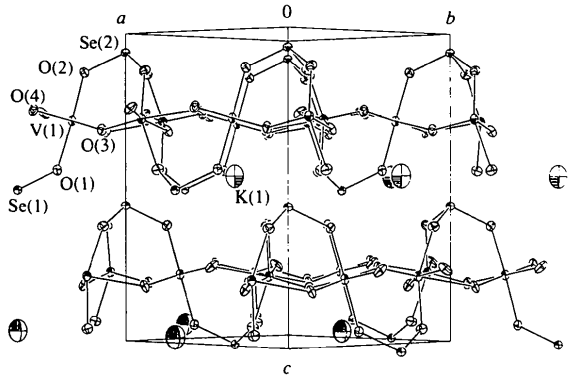

Fig. 2. View approximately down [110] of the $K(VO_2)_3(SeO_3)_2$ structure, showing the doubly capped V/Se/O sheets, and inter-layer K cations. Displacement ellipsoids are drawn at the 50% probability level.

The V/Se/O layers have an *ABAB* repeat motif in the crystallographic *z* direction. Since adjacent layers are staggered with respect to one another, there are no pseudo-one-dimensional channels in this structure comparable with the infinite [001] channels found in hexagonal WO_3-type materials (Figlarz, 1989). This layer-staggering also results in the Se atoms having different environments: the Se(1) atom is positioned towards a six-ring hole in the next V/Se/O layer, whereas the Se(2) atom is projected towards an uncapped three-ring hole in the adjacent layer.

The geometry of the VO_6 entity in $K(VO_2)_3(SeO_3)_2$ is distorted from regular octahedral, with the V atom showing a displacement from the geometrical center of its six O-atom neighbors towards an octahedral edge. This displacement, by 0.37 Å, results in two short (< 1.66 Å) V—O bonds in *cis* configuration, both of which are *trans* to long V—O links (> 2.17 Å). These four V—O bonds provide the in-sheet inter-vanadium connectivity. Two V—O bonds of intermediate length (1.90–2.00 Å) make up the VO_6 unit. Both of these latter bonds form part of the V—O—Se linkages. This VO_6 distortion, which may be viewed as a tendency towards tetrahedral geometry, is unusual compared with the more common local vanadium(V) atomic displacement towards an octahedral vertex, which results in one short 'vanadyl' V=O bond (< 1.65 Å), a long *trans* V—O link, and four intermediate-length V—O bonds (Gopal & Calvo, 1972). Despite this atypical vanadium coordination, which was also observed for the vanadium species in $NH_4(VO_2)_3(SeO_3)_2$ (Vaughey *et al.*, 1994), the bond-valence sum (BVS) value of 5.14 for this atom is typical for vanadium(V) (Brese & O'Keeffe, 1991).

Both Se atoms in $K(VO_2)_3(SeO_3)_2$ occupy special positions with 3.. site symmetry. Their pyramidal bonding geometry and Se—O bond lengths are typical, and similar to those observed for the corresponding species in $NH_4(VO_2)_3(SeO_3)_2$. The K cation in $K(VO_2)_3(SeO_3)_2$ (site symmetry 3..) is sixfold coordinated by O-atom neighbors in a distorted trigonal-prismatic configuration. This atom is significantly 'underbonded', based on BVS calculations {BVS[K(1)] = 0.43, compared with an expected value of 1.00}, and its thermal parameters are relatively large. It is notable that the inter-layer separations (defined by half the *c* unit-cell dimension) in $K(VO_2)_3(SeO_3)_2$ and $NH_4(VO_2)_3(SeO_3)_2$ are almost identical: 5.70 Å for the K phase, and 5.73 Å for the NH_4 phase.

$K(VO_2)_3(SeO_3)_2$ and $NH_4(VO_2)_3(SeO_3)_2$ (Vaughey *et al.*, 1994) may be compared with the molybdenum(IV)-containing phases $(NH_4)_2(MoO_3)_3SeO_3$ and $Cs_2(MoO_3)_3SeO_3$ (Harrison, Dussack & Jacobson, 1994), which are built up from HTO-like corner-sharing MoO_6 layers. In these $M_2(MoO_3)_3SeO_3$ phases, the infinite Mo/O layers are capped by Se atoms on one side of the sheet only, as opposed to the Se capping on both sides that occurs in the vanadium-containing materials.

Experimental

$K(VO_2)_3(SeO_3)_2$ was prepared hydrothermally from 0.3 g of V_2O_5 (3.3 mmol vanadium), 1.098 g of SeO_2 (9.9 mmol selenium), and 0.228 g of K_2CO_3 (3.3 mmol potassium) (*i.e.* starting K:V:Se ratio = 1:1:3). This mixture was dissolved in 8 ml of H_2O and heated in a 23 ml teflon-lined Parr hydrothermal bomb at 473 K for 4 d. Solid-product recovery (96% yield by weight, based on vanadium) yielded light-green hexagonal rods of the title compound, which were coated by a thin layer of unidentified orange material. This orange layer was removed by sonication for 1 h in deionized water.

Thermogravimetric analysis of $K(VO_2)_3(SeO_3)_2$ showed a clean one-step 40.9% weight loss between 553 and 653 K (calculated weight loss for sublimation of all selenium as SeO_2 = 41.0%). After heating to 773 K in oxygen, the resulting rust-brown powder, of overall nominal stoichiometry KV_3O_8,

yielded a poorly crystalline pattern. Some of the lines in this pattern correspond to those for the phase described as $K_{0.51}V_2O_5$ (Vandenborre, Sanchez & Politi, 1985). Further heating to 1073 K resulted in a clean sharp $K_{0.51}V_2O_5$ pattern.

The IR spectrum (KBr pellet method) of $K(VO_2)_3(SeO_3)_2$ is featureless in the region 4000–1000 cm^{-1}. Bands at 945, 806 and 685 cm^{-1} may be equated with similar features in the IR spectrum of $NH_4(VO_2)_3(SeO_3)_2$ (Vaughey *et al.*, 1994).

Crystal data

$K(VO_2)_3(SeO_3)_2$
M_r = 541.84
Hexagonal
$P6_3$
a = 7.121 (4) Å
c = 11.400 (7) Å
V = 500.6 (5) Å^3
Z = 2
D_x = 3.60 Mg m^{-3}
Mo $K\alpha$ radiation
λ = 0.7107 Å
Cell parameters from 25 reflections
θ = 10–18°
μ = 10.34 mm^{-1}
T = 298 K
Hexagonal column
0.35 × 0.30 × 0.30 mm
Light green

Data collection

Enraf–Nonius CAD-4 automated diffractometer
ω–2θ scans
Absorption correction: ψ scans
T_{min} = 0.10, T_{max} = 0.14
1193 measured reflections
972 independent reflections
972 observed reflections [$F > 0$]
R_{int} = 0.011
θ_{max} = 30.0°
$h = -8 \rightarrow 0$
$k = 0 \rightarrow 10$
$l = -16 \rightarrow 16$
3 standard reflections
frequency: 10 000 s
intensity decay: none

Refinement

Refinement on F
R = 0.035
wR = 0.027
S = 1.07
972 reflections
57 parameters
Tukey–Prince weighting scheme, fitted using a three-term Chebychev polynomial (Carruthers & Watkin, 1979)
$(\Delta/\sigma)_{max}$ = 0.01
$\Delta\rho_{max}$ = 2.0 e Å^{-3}
$\Delta\rho_{min}$ = −1.7 e Å^{-3}
Extinction correction: Larson (1970)
Extinction coefficient: 24 (2)
Atomic scattering factors from *International Tables for X-ray Crystallography* (1974, Vol. IV, Table 2.2B)
Absolute configuration: Flack (1983) parameter = 0.05 (2) (see below)

Table 1. *Fractional atomic coordinates and equivalent isotropic displacement parameters* (Å^2)

$$U_{eq} = (1/3)\Sigma_i\Sigma_j U_{ij} a_i^* a_j^* \mathbf{a}_i.\mathbf{a}_j.$$

	x	y	z	U_{eq}
K(1)	1/3	2/3	−0.0345 (3)	0.0576
V(1)	0.7863 (1)	0.1200 (1)	−0.21654 (9)	0.0111
Se(1)	1/3	2/3	0.51033 (8)	0.0108
Se(2)	0	0	0.06094 (9)	0.0110
O(1)	0.8010 (6)	0.2193 (6)	−0.0535 (3)	0.0150
O(2)	0.8835 (6)	0.1344 (6)	−0.3745 (3)	0.0147
O(3)	0.7441 (5)	−0.1233 (5)	−0.1829 (3)	0.0130
O(4)	0.5401 (6)	0.0743 (7)	−0.2458 (3)	0.0156

Table 2. *Selected geometric parameters* (Å, °)

K(1)···O(2^i)	3.147 (4)	V(1)—O(3^{vii})	2.186 (3)
K(1)···O(2^{ii})	3.147 (4)	V(1)—O(4)	1.649 (4)
K(1)···O(2^{iii})	3.147 (4)	V(1)—O(4^{viii})	2.172 (4)
K(1)···O(3^{iv})	3.046 (4)	Se(1)—O(1^i)	1.697 (4)
K(1)···O(3^v)	3.046 (4)	Se(1)—O(1^{ii})	1.697 (4)
K(1)···O(3^{vi})	3.046 (4)	Se(1)—O(1^{iii})	1.697 (4)
V(1)—O(1)	1.972 (3)	Se(2)—O(2^{ix})	1.715 (3)
V(1)—O(2)	1.913 (4)	Se(2)—O(2^x)	1.715 (3)
V(1)—O(3)	1.648 (3)	Se(2)—O(2^{iii})	1.715 (3)
O(1)—V(1)—O(2)	156.1 (2)	O(3^{vii})—V(1)—O(4^{viii})	75.5 (2)
O(1)—V(1)—O(3)	96.1 (3)	O(4)—V(1)—O(4^{viii})	91.8 (4)
O(2)—V(1)—O(3)	98.4 (3)	O(1^i)—Se(1)—O(1^{ii})	103.0 (2)
O(1)—V(1)—O(3^{vii})	80.2 (2)	O(1^i)—Se(1)—O(1^{iii})	103.0 (2)
O(2)—V(1)—O(3^{vii})	81.0 (2)	O(1^{ii})—Se(1)—O(1^{iii})	103.0 (2)
O(3)—V(1)—O(3^{vii})	89.8 (3)	O(2^{ix})—Se(2)—O(2^x)	102.9 (2)
O(1)—V(1)—O(4)	97.0 (2)	O(2^{ix})—Se(2)—O(2^{iii})	102.9 (2)
O(2)—V(1)—O(4)	98.1 (2)	O(2^x)—Se(2)—O(2^{iii})	102.9 (2)
O(3)—V(1)—O(4)	102.9 (2)	V(1)—O(1)—Se(1^{xi})	129.4 (3)
O(3^{vii})—V(1)—O(4)	167.3 (2)	V(1)—O(2)—Se(2^{xi})	129.6 (3)
O(1)—V(1)—O(4^{viii})	80.0 (2)	V(1)—O(3)—V(1^{xii})	140.2 (3)
O(2)—V(1)—O(4^{viii})	81.2 (2)	V(1)—O(4)—V(1^{vi})	140.8 (3)
O(3)—V(1)—O(4^{viii})	165.3 (3)		

Symmetry codes: (i) $x-y, x, \frac{1}{2}+z$; (ii) $1-x, 1-y, \frac{1}{2}+z$; (iii) $y, 1-x+y, \frac{1}{2}+z$; (iv) $x, 1+y, z$; (v) $-y, x-y, z$; (vi) $1-x+y, 1-x, z$; (vii) $2-x+y, 1-x, z$; (viii) $1-y, x-y, z$; (ix) $x-y-1, x-1, \frac{1}{2}+z$; (x) $1-x, -y, \frac{1}{2}+z$; (xi) $1+x-y, x, z-\frac{1}{2}$; (xii) $1-y, x-y-1, z$.

The absolute structure of the individual crystal of $K(VO_2)_3(SeO_3)_2$ studied was determined by refining the Flack (1983) polarity parameter, and is as defined by Table 1. Refinement of a model of the opposite enantiomer of $K(VO_2)_3(SeO_3)_2$ (Flack parameter fixed at 1.00) resulted in final residuals of R = 0.058 and wR = 0.053. We assume that the as-synthesized $K(VO_2)_3(SeO_3)_2$ consists of a random 50:50 mixture of both enantiomers. Further measurements are required to establish the connection between each enantiomer and its macroscopic physical properties. The maximum in the final Fourier difference map (2.0 e Å^{-3}) was found within 0.83 Å of O(4), and the minimum (−1.7 e Å^{-3}) was found 0.73 Å away from Se(2).

Data collection: *CAD-4 Software* (Enraf–Nonius, 1989). Cell refinement: *CAD-4 Software*. Data reduction: *RC*85 (Baird, 1985). Program(s) used to refine structure: *CRYSTALS* (Watkin, Carruthers & Betteridge, 1990). Molecular graphics: *ORTEP*II (Johnson, 1976). Software used to prepare material for publication: local routines.

We thank the National Science Foundation (DMR921-4804) and the Robert A. Welch Foundation for partial financial support.

Lists of structure factors, anisotropic displacement parameters and complete geometry have been deposited with the IUCr (Reference: BR1110). Copies may be obtained through The Managing Editor, International Union of Crystallography, 5 Abbey Square, Chester CH1 2HU, England.

References

Baird, P. D. (1985). *RC*85 *User Guide*. Univ. of Oxford, England.
Brese, N. E. & O'Keeffe, M. (1991). *Acta Cryst.* B**47**, 192–197.
Carruthers, J. R. & Watkin, D. J. (1979). *Acta Cryst.* A**35**, 698–699.
Enraf-Nonius (1989). *CAD-4 Software*. Version 5.0. Enraf-Nonius, Delft, The Netherlands.
Figlarz, M. (1989). *Prog. Solid State Chem.* **19**, 1–46.

Flack, H. D. (1983). *Acta Cryst.* A**39**, 876–881.
Gopal, R. & Calvo, C. (1972). *J. Solid State Chem.* **5**, 432–435.
Harrison, W. T. A., Dussack, L. L. & Jacobson, A. J. (1994). *Inorg. Chem.* **33**, 6043–6049.
Johnson, C. K. (1976). *ORTEP*II. Report ORNL-5138. Oak Ridge National Laboratory, Tennessee, USA.
Larson, A. C. (1970). *Crystallographic Computing*, edited by F. R. Ahmed, S. R. Hall & C. P. Huber, pp. 291–294. Copenhagen: Munksgaard.
Vandenborre, M., Sanchez, C. & Politi, A. (1985). *Nouv. J. Chem.* **9**, 511–518.
Vaughey, J. T., Harrison, W. T. A., Dussack, L. L. & Jacobson, A. J. (1994). *Inorg. Chem.* **33**, 4370–4375.
Watkin, D. J., Carruthers, J. R. & Betteridge, P. W. (1990). *CRYSTALS User Guide*. Chemical Crystallography Laboratory, Univ. of Oxford, England.

Acta Cryst. (1995). C**51**, 2476–2477

Low-Density Form of $NaGaSi_2O_6$

HARUO OHASHI, TOSHIKAZU OSAWA AND AKIRA SATO

National Institute for Research in Inorganic Materials, Namiki 1-1, Tsukuba, Ibarki 305, Japan

(*Received* 12 *December* 1994; *accepted* 13 *June* 1995)

Abstract

The structure of the title compound, gallium sodium silicate, is similar to that of jadeite ($NaAlSi_2O_6$). Comparison of the new crystal-structure refinement for $NaGaSi_2O_6$ with published refinements for eleven $NaM^{3+}Si_2O_6$ pyroxenes suggests that there are two different electronic states, Ga(α) and Ga(β), for the octahedral Ga^{3+} ion. Ga(α) occurs in the Mn–Fe–Ga(α) series and Ga(β) in the Al–Ga(β)–In series.

Comment

The structure of the title compound is isostructural with $NaAlSi_2O_6$, $NaCrSi_2O_6$ and $NaFeSi_2O_6$ (Clark, Appleman & Papike, 1969), $NaScSi_2O_6$ (Hawthorne & Grundy, 1973), $NaInSi_2O_6$ (Hawthorne & Grundy, 1974), $NaTiSi_2O_6$ (Ohashi, Fujita & Osawa, 1982), Na Ga(α)Si_2O_6 (Ohashi, Fujita & Osawa, 1983) $NaMnSi_2O_6$ (Ohashi, Osawa & Tsukimura, 1987) and $NaVSi_2O_6$ (Ohashi, Osawa & Sato, 1994).

The cell parameters of the Na Ga(α)Si_2O_6 pyroxene are: a = 9.557 (5), b = 8.679 (4), c = 5.260 (1) Å, β = 107.68 (2)° and V = 415.7 (3) Å^3 (Ohashi *et al.*, 1983). The calculated density (D_x) is 3.91 Mg m^{-3} and is higher than that (D_x = 3.89 Mg m^{-3}) of the Na Ga(β)Si_2O_6 pyroxene studied here. The atomic z coordinate for O1 [z = 0.1312 (7)] of the Na Ga(α)Si_2O_6 pyroxene differs from that of the Na Ga(β)Si_2O_6 pyroxene.

The O1—Si—O2 angle is the largest O—Si—O angle in the $NaM^{3+}Si_2O_6$ pyroxenes. This may be due in part to the greater repulsion between the more negatively charged non-bridging O atoms. As shown in Fig. 2, the O1—Si—O2 angles correlate with the differences d_{br-nbr} in such a way that they follow three different trends: the Sc–Ti–V–Cr series, the Mn–Fe–Ga(α) series and the Al–Ga(β)–In series, where d_{br-nbr} = ⟨Si—O_{br}⟩ − ⟨Si—O_{nbr}⟩ (br = bridging, nbr = non-bridging), ⟨Si—O_{br}⟩ = 1/2(Si—O3*A*1 + Si—O3*A*2)

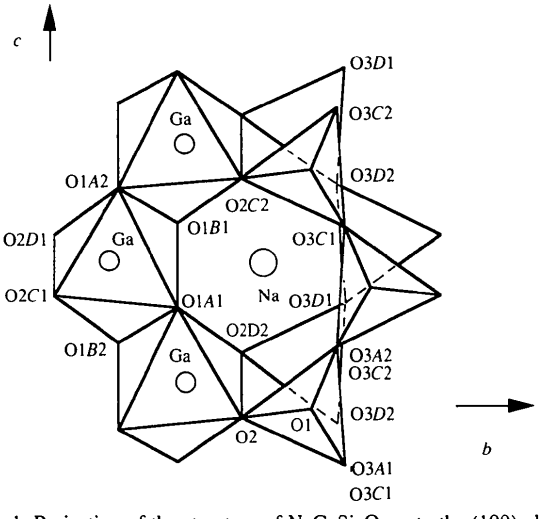

Fig. 1. Projection of the structure of $NaGaSi_2O_6$ onto the (100) plane. Atom labelling follows that used by Clark *et al.* (1969).

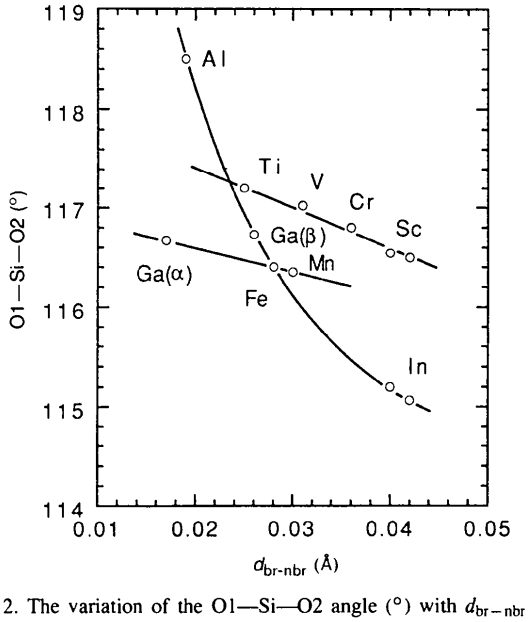

Fig. 2. The variation of the O1—Si—O2 angle (°) with d_{br-nbr} (Å) for the $NaM^{3+}Si_2O_6$ pyroxenes. Data are from Ohashi *et al.* (1994).